Quantum-to-classical limit of a dynamically driven spin

L. E. Ballentine
Department of Physics, Simon Fraser University, Burnaby, British Columbia, Canada V5A 1S6
(Received 12 November 1992)

Classical and quantum models of a localized spin driven by a polarized-spin beam have been shown to exhibit a rich variety of dynamical behaviors. In the classical model these include stable limit points, limit cycles, and chaos; however, in the quantum model the density matrix of the localized spin generally approaches a steady state. This paradox is resolved by considering the autocorrelation functions of the spin components, which reveal the expected quantum-classical correspondence. The noncommuting of the limits $j\to\infty$ and $t\to\infty$ is explained in this model by the limiting behavior of certain eigenvalue distributions, and the significance of these limits is discussed. The study also highlights the unresolved problem of interpreting the complex correlation functions of noncommuting operators.

PACS number(s): 03.65.−w, 03.20.+i, 05.45.+b

I. INTRODUCTION

In a pair of papers, [1] and [2], the concept of *dynamical driving* was defined as the driving of a system by another dynamical system. It was anticipated that dynamical driving would yield a richer variety of motions than driving by an *external force,* which acts on the system but is not reacted upon by the system.

The model (see [1] for more details) consists of a localized spin j_1, a beam of spins j_2 polarized in the y direction, and a magnetic field B in the z direction. The beam particles interact, one at a time, with the localized spin, and so the effect of one beam particle on the state of the localized spin can be treated as a discrete mapping. While a beam particle is in the interaction region, for a duration τ, the Hamiltonian of the two interacting spins is

$$H_{12}=a(\mathbf{S}_1\cdot\mathbf{S}_2)+\mathbf{B}\cdot(\mathbf{S}_1+\mathbf{S}_2)\ . \tag{1}$$

The beam affects the localized spin by transferring angular momentum to it, so the interaction tends to polarize the localized spin in the y direction. The magnetic field rotates any such polarization about the z axis. It is surprising that competition between these two effects yields such a rich variety of behaviors in a simple model. In the classical version of this model, the motion of the localized spin exhibits stable attractors, bifurcations, limit cycles, and chaos. The quantal model also shows a rich variety of behaviors, some being analogs of classical motions, and others being purely quantum mechanical.

Papers [1] and [2] concentrated upon the nature of the steady state that is ultimately reached. (The term "steady state" is used here to include periodic, quasiperiodic, and chaotic attractors, as well as fixed points.) In this paper we shall focus on the dynamics of the motion, and especially on the quantum-to-classical limits.

Dynamical driving has also been studied in the Jaynes-Cummings model of a two-level atom interacting with an electromagnetic field mode. Slosser, Meystre, and Braunstein [3] considered the field mode as the driven system, with a beam of two-level atoms providing the driving. On the other hand, Gea-Banacloche [4] studied the states of the atom, with the field mode acting as the driver. These models exhibit both similarities to and differences from the spin model of this paper.

II. DYNAMICS OF THE MODEL

A. The need to study correlation functions

The need to introduce correlation functions can be illustrated by some results obtained in [2]. Figure 1 shows a portion of the phase diagram of the final states for the classical model. It corresponds to the value $B=\pi$ (in units $\hbar=1$, $\tau=1$), such that the effect of the magnetic field during the interaction time τ is to rotate the spins through the angle π. In this case, the longitudinal component (parallel to the beam) of the localized spin $\mathbf{S}_1$ is decoupled from its transverse components, and so it is sufficient to discuss the behavior of the longitudinal (y) component. If $\mathbf{S}_1$ is parallel (or antiparallel) to the beam spins, then the interaction $(\mathbf{S}_1\cdot\mathbf{S}_2)$ is a minimum (or maximum) and no torque is exerted on the localized spin by the beam. Thus the localized spin merely flips back and forth between $Y=+1$ and -1 under the action of the magnetic field. (Y is the y component of $\mathbf{S}_1/j_1$.) This period-2 cycle is the unique steady state within the region marked $Y=\{+1,-1\}$ in Fig. 1; elsewhere it is unstable.

Consider now the corresponding quantum-mechanical model for the same range of parameters. It was shown in [1] that the density matrix of the localized spin approaches a time-independent steady state. In the limit of large j_1, the probability distribution for the y component of $\mathbf{S}_1$ becomes bimodal, with narrow peaks at $\pm j_1$ (see Fig. 14 of [2]). This is in agreement with the time ensemble for the classical steady state, but it gives no indication of the classical period-2 oscillation. However, this contradiction between the classical model and the $j_1\to\infty$ limit of the quantum model (period-2 oscillation versus a time-independent steady state) is only apparent. For an arbitrary initial state of the classical model (with parameters in the region marked $Y=\{+1,-1\}$ in Fig. 1), we

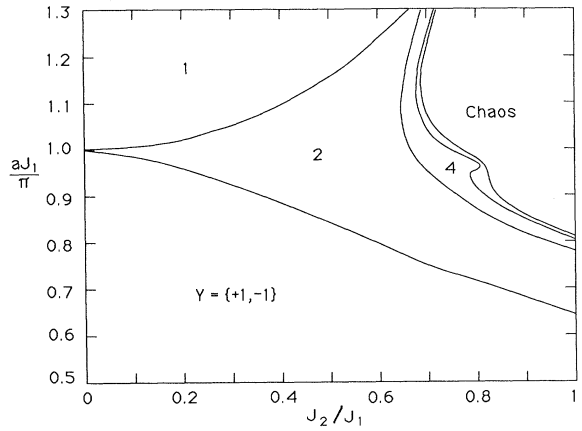

FIG. 1. $B=\pi$ phase diagram for the Y component of the localized spin (from [2]).

know not only that spin is equally likely to point in either of the directions $Y=+1$ or -1, but also that it alternates between them. To obtain the corresponding information for the quantum model, we must calculate a correlation function such as $\langle S_y(t)S_y(t+\tau)\rangle$. These correlation functions contain information about the dynamics, notwithstanding the stationary character of the state function.

B. Equations of motion

The Hamiltonian for the whole system, consisting of the localized spin and the beam, is time dependent because each beam particle interacts with the localized spin only while it is in the interaction region. For example, as the first three beam particles enter and leave the interaction region the Hamiltonian takes on the following forms:

$$\begin{aligned} H(t)&=H_{01}\otimes I\otimes I\otimes\cdots \quad (0<t<\tau)\ , \\ &=I\otimes H_{02}\otimes I\otimes\cdots \quad (\tau<t<2\tau)\ , \\ &=I\otimes I\otimes H_{03}\otimes\cdots \quad (2\tau<t<3\tau)\ . \end{aligned} \tag{2}$$

Here the places in the tensor product represent the successive beam particles, and the subscript zero refers to the localized spin. Each of the two-particle interaction factors are of the form (1). The time development operator from $t=0$ to $n\tau$, describing the effect of n beam particles passing through the interaction region, has the form

$$U(n\tau,0)=U(n\tau,(n-1)\tau)\cdots U(2\tau,\tau)U(\tau,0)\ , \tag{3}$$

where each of the factors on the right-hand side of (3) is an exponential function of the appropriate form of $H(t)$ in (2).

The effect of one beam particle (entering at time t and leaving at time $t+\tau$) on the state operator of the whole system ρ_s is

$$\rho_s(t+\tau)=U(t+\tau,t)\rho_s(t)U^\dagger(t+\tau,t)\ . \tag{4}$$

The initial state of the two interacting particles will be of the form

$$\rho_s(t)=\rho_l(t)\otimes\rho_b\ , \tag{5}$$

where $\rho_l(t)$ is the initial state of the localized spin, and ρ_b is the initial state of the beam particle. We are interested only in the localized spin, discarding each beam particle after interaction, so it is sufficient to consider only the *partial state* of the localized spin (also called the *reduced state*),

$$\rho_l(t+\tau)=\mathrm{Tr}^{(b)}\rho_s(t+\tau)\ , \tag{6}$$

obtained by tracing over the coordinates of the beam particle. Thus the effect of one beam particle on the density matrix of the localized spin is a linear transformation,

$$\begin{aligned} \langle a|\rho_l(t+\tau)|b\rangle &= \sum_\alpha\sum_{c,\gamma}\sum_{d,\delta}\langle a\alpha|U|c\gamma\rangle\langle c|\rho_l(t)|d\rangle \\ &\quad\times\langle\gamma|\rho_b|\delta\rangle\langle d\delta|U^\dagger|b\alpha\rangle \\ &= \sum_{c,d}M_{ab;cd}\langle c|\rho_l(t)|d\rangle\ . \end{aligned} \tag{7}$$

The dynamics of the localized spin is obtained by iteration of a linear mapping,

$$\rho_l(t+\tau)=M\rho_l(t)\ , \tag{8}$$

where the "matrix" M, defined implicitly by (7), is a four-dimensional array and the "vector" ρ_l is a two-dimensional array. The eigenvalues and eigenvectors of M,

$$M\rho_\Lambda=\Lambda\rho_\Lambda\ , \tag{9}$$

determine possible dynamical behaviors. An eigenvector ρ_Λ with $\Lambda=1$ describes a steady state. An eigenvector with $|\Lambda|<1$ describes a decaying transient. $|\Lambda|>1$ is impossible, since exponential growth would violate the condition $\mathrm{Tr}\rho^2\le 1$. An oscillatory limit cycle would occur if $|\Lambda|=1$, $\Lambda\neq 1$, although no such case has been found for this model. Except for certain special values of the parameters (a set of measure zero), it has been found that there is *exactly one* eigenvalue $\Lambda=1$, so the state of the localized spin goes to a *unique* final steady state.

In the above discussion, we used the Schrödinger picture, with a time-dependent state function $\rho_s(t)$. In order to discuss *correlation functions,* it is necessary to use the *Heisenberg picture,* with a time-independent state function and time-dependent observables. Therefore we introduce two Heisenberg operators (in practice these will be spin components),

$$Q(t_1)=U^\dagger(t_1,0)QU(t_1,0)\ , \tag{10}$$

$$R(t_2)=U^\dagger(t_2,0)RU(t_2,0)\ , \tag{11}$$

and their correlation function,

$$\langle Q(t_1)R(t_2)\rangle=\mathrm{Tr}\{\rho_s(0)Q(t_1)R(t_2)\}\ . \tag{12}$$

For $t_2>t_1$, we may write $U(t_2,0)=U(t_2,t_1)U(t_1,0)$. Substituting this into (12), and performing a cyclic permutation of the operators whose trace is being taken, we obtain

$$\langle Q(t_1)R(t_2)\rangle=\mathrm{Tr}\{\rho_s(t_1)QR_1(t_2-t_1)\}\ , \tag{13}$$

where $\rho_s(t_1)=U(t_1,0)\rho_s(0)U^\dagger(t_1,0)$ and Q are ordinary Schrödinger-picture operators, and

$$R_1(t_2-t_1)=U^\dagger(t_2,t_1)RU(t_2,t_1) \tag{14}$$

is a Heisenberg-picture operator referred to the origin $t=t_1$.

We shall assume that Q and R represent dynamical variables of the localized spin, i.e., that they operate only in the Hilbert space of the localized spin. Then in (13) we may trace over all the variables pertaining to the beam particles that have passed through the apparatus before $t=t_1$, effectively reducing the many-particle density matrix $\rho_s(t_1)$ to the localized-spin density matrix $\rho_l(t_1)$ [as calculated from (7) and (8)]. Because of the interactions, the operator $R_1(t_2-t_1)$ contains correlations between the Hilbert spaces of the localized spin and the beam particles that pass through the apparatus between $t=t_1$ and t_2. But one can trace over the variables of those beam particles, and obtain an equation, similar to (7), for an operator $R_{1l}(t_2-t_1)$ that is reduced to the Hilbert space of the localized spin. The result is

$$\langle a|R_{1l}(t+\tau)|b\rangle=\sum_{c,d}M_{dc;ba}\langle c|R_{1l}(t)|d\rangle\ , \tag{15}$$

which can be solved recursively, beginning with $R_{1l}(0)=R$. Finally, the evaluation of (13) is completed by a trace over the variables of the localized spin,

$$\langle Q(t_1)R(t_2)\rangle=\mathrm{Tr}^{(l)}\{\rho_l(t_1)QR_{1l}(t_2-t_1)\}\ . \tag{16}$$

The matrix $M_{dc,ba}$ that occurs in (15) is the transpose of the matrix in (7), the difference being due to the different order of the operators $U^\dagger$ and U in (4) and (11). The eigenvalues computed from (9) are also relevant to (15) because a matrix has the same eigenvalues as does its transpose. If Eq. (8) is iterated until the density matrix reaches its steady-state value, $\rho_l(\infty)$, then the correlation function $\langle Q(t_1)R(t_2)\rangle$ will be a function only of t_2-t_1, and its time dependence will be directly related to the eigenvalues of M in (9).

C. Interpretation of correlation functions

Correlation functions like $\langle Q(t_1)R(t_2)\rangle$ bring us face to face with an old question in the interpretation of quantum mechanics, to which no definitive answer has ever been given. What is the meaning of such a correlation function if the two operators do not commute? There is no difficulty if the operators commute. Then they possess a complete set of common eigenvectors, from which a non-negative joint-probability distribution can be computed, and the correlation function is just the average of the product of the simultaneous eigenvalues of the two dynamical variables with that joint-probability distribution. But if the operators do not commute, then no such set of eigenvectors exists. One can use the spectral projectors of the noncommuting operators to give an apparently natural definition to their joint distributions [5], but the resulting distributions take on negative values, and so they have no probability interpretation. Moreover, the correlation function (12) is generally complex,

$$\langle Q(t_1)R(t_2)\rangle=\tfrac{1}{2}\langle Q(t_1)R(t_2)+R(t_2)Q(t_1)\rangle -\tfrac{1}{2}\langle[Q(t_1),R(t_2)]\rangle\ , \tag{17}$$

the symmetrized term giving the real part, and the commutator giving the imaginary part.

The "orthodox" response to this problem has been to assert that two dynamical variables cannot be simultaneously measured if their operators do not commute, therefore one should not discuss their correlations. Regardless of the truth or otherwise of the premise of this argument, the conclusion is quite beside the point. In fact, correlation functions like (17) arise naturally as the fundamental constituents of a dynamical theory, regardless of their measurability [6]. Moreover, one must be able to define a quantum correlation function in order to make contact with classical correlations in the appropriate limit.

The orthodox view is also unsatisfactory because of its instability under small perturbations. If the commutator is *exactly* zero, then a correlation function with a normal statistical interpretation exists. But what if the imaginary part of (17) is several orders of magnitude smaller than the real part (as indeed happens in many of the cases studied in this paper)? The orthodox view denies any meaning to a correlation function in such a case, whereas common sense suggests that there should be some continuity between the commutative and noncommutative cases.

I offer no solution to this old problem, but in order to proceed I shall assume that the real part of (17) can be regarded as the quantum correspondent of the classical correlation function. This assumption is reasonable, but it stands in need of a more fundamental justification. The often-expressed view, that problems in the interpretation of quantum mechanics are merely "philosophy," is contradicted by this case; indeed the failure to solve such problems can obstruct progress in "normal" science.

III. EIGENVALUE DISTRIBUTIONS

The dynamical behavior of the quantum system is characterized by the eigenvalues of (9), so it is of interest to see whether the form of this eigenvalue spectrum is related to the classical motion. There is a well-established theory connecting the eigenvalue spectrum of a quantum Hamiltonian with the classical periodic orbits [7], but it is not applicable to the matrix M in (9), which is neither Hermitian nor unitary. Figures 2–5 show the eigenvalue spectra for four sets of parameters, corresponding to four qualitatively different classical motions. The parameters for Fig. 2 lie in the phase marked $Y=\pm1$ in Fig. 1; those for Fig. 3 lie in the "chaos" phase; those for Fig. 4 lie in the phase marked "1," for which the y component of the localized spin converges to a steady value while the x and z components move on a limit cycle transverse to the beam. Figure 5, for $B=0.7\pi$ (not in Fig. 1), corresponds to a classical motion having two distinct attractors. Clearly the patterns are very different for the different kinds of classical motions. The patterns are qualitatively similar at different points within the same phase in Fig. 1, for example, different parameter values within the phase $Y=\pm1$ lead to eigenvalues that cluster near the real axis.

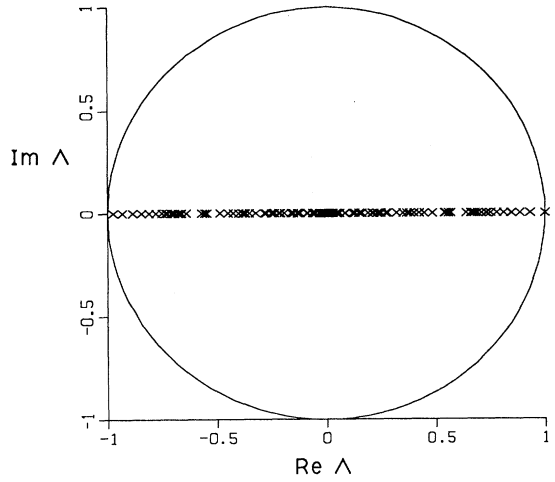

FIG. 2. Complex eigenvalues for $j_1=6$, $j_2=3$, $aj_1=\pi/2$, $B=\pi$. (Corresponding classical phase in Fig. 1 is $Y=\pm 1$.)

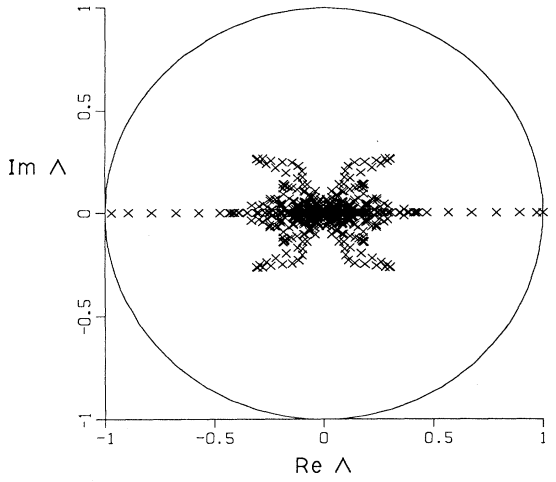

FIG. 4. Complex eigenvalues for $j_1=12$, $j_2=6$, $aj_1=1.5\pi$, $B=\pi$. (Corresponding classical phase in Fig. 1 is 1.)

However, the patterns vary continuously across phase boundaries, there being no discontinuous phase transitions for finite values of j_1 and j_2.

The statistical distributions of energy eigenvalues have been shown to be related to the nature (integrable or chaotic) of the corresponding classical motion [8]. In particular, "repulsion" of neighboring eigenvalues has been identified as a common signature of chaos. This concept has also proved useful for the complex eigenvalues of the Fokker-Planck equation [9]. However, Figs. 2–5 indicate no apparent applicability of such ideas to the eigenvalues of Eq. (9).

The number of eigenvalues in each figure is $(2j_1+1)^2$, and many near the origin are not resolved. (This contrasts with the results of Ref. [8], Sec. 8.6, for dissipative quantum maps, whose complex eigenvalues are confined to an annulus that excludes the origin.) Although the eye is drawn to the complex pattern of eigenvalues near the center of the picture, those represent short-lived transients. It is the eigenvalues on or near the unit circle that are most significant. In all of these cases there is a single eigenvalue on the unit circle, $\Lambda=1$, that corresponds to the steady state. In Fig. 2 the nearest eigenvalue to the unit circle (called the *subdominant* eigenvalue) is $\Lambda\approx -1$, corresponding to a pole-to-pole ($Y=\pm 1$) oscillation of the spin polarization. The oscillation is damped because $|\Lambda|<1$, but as j_1 increases Λ rapidly approaches -1 (see Fig. 6). Thus in the limit $j_1\to\infty$ the pole-to-pole oscillation becomes undamped, as in the classical model.

There is a well-known conjecture (rigorously proven in some cases [10]) which asserts that the limits $\hbar\to 0$ and $t\to\infty$ cannot be interchanged. For spin models, the lim-

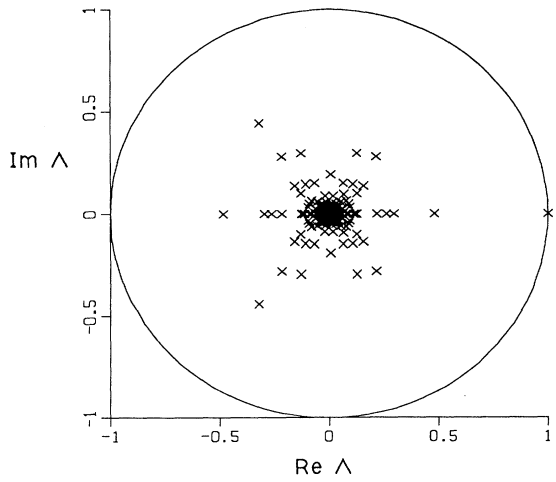

FIG. 3. Complex eigenvalues for $j_1=12$, $j_2=12$, $aj_1=\pi$, $B=\pi$. (Corresponding classical phase in Fig. 1 is chaos.)

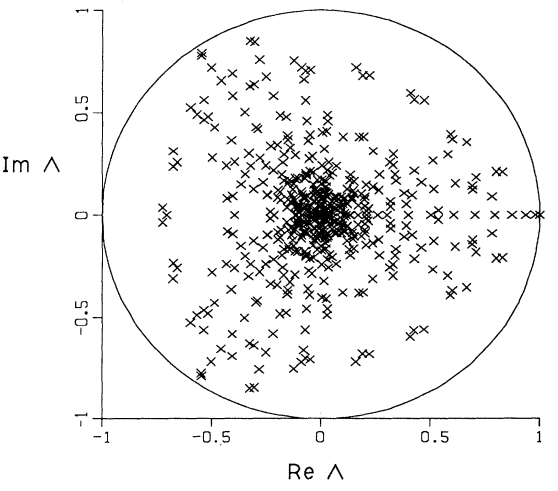

FIG. 5. Complex eigenvalues for $j_1=12.5$, $j_2=2.5$, $aj_1=\pi$, $B=0.7\pi$. (Corresponding classical phase has two basins of attraction.)

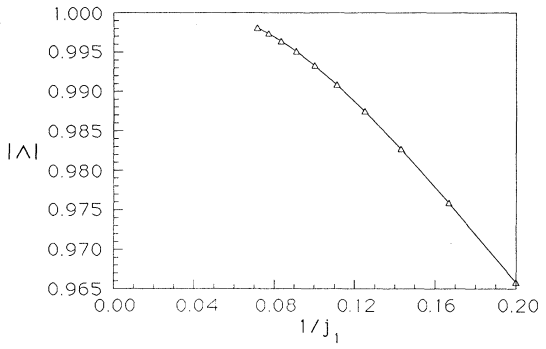

FIG. 6. Magnitude of the subdominant eigenvalue ($\Lambda \approx -1$, as in Fig. 2) vs $1/j_1$, for $j_2/j_1=0.5$, $aj_1=\pi/2$, $B=\pi$.

it $\hbar \to 0$ becomes $j \to \infty$, since the macroscopic angular momentum, $\hbar j$, must be held constant in the "classical" limit. Now for any value of j_1, the $t \to \infty$ limit is determined by the eigenvectors (usually only one) corresponding to $|\Lambda|=1$. The limit $t \to \infty$ can fail to commute with the limit $j_1 \to \infty$ only if one or more eigenvalues converge onto the unit circle from within as $j_1 \to \infty$. That this happens for parameters within the phase $Y=\pm 1$ is clearly shown by Fig. 6. But for the chaos phase, the eigenvalues (Fig. 3) behave very differently. Figure 7 shows the variation of $|\Lambda|$ with j_1 for the closest real and complex eigenvalues to the unit circle, and although $|\Lambda|$ increases with j_1, it shows no sign of approaching unity. If these trends, which appear well established in Fig. 7, continue indefinitely, then the conjecture must be false in the region of chaos (although true in the phase $Y=\pm 1$). If, in spite of appearances to the contrary, the conjecture remains true in the region of chaos, then the behavior of the eigenvalues must change radically for larger values of j_1. Indeed, a comparison of Figs. 6 and 7 suggests that for the subdominant eigenvalue to reach $|\Lambda|=0.999$, it would require orders-of-magnitude larger values of j_1 in the chaos phase than are needed in the phase $Y=\pm 1$.

IV. AUTOCORRELATION FUNCTIONS

The dynamics of the localized spin can be studied by means of the autocorrelation functions for its components, such as $\langle S_y(t_1)S_y(t_2)\rangle$. We shall evaluate them for the final steady state, in which they depend upon only the time difference, $t=t_2-t_1$. It is convenient to subtract the large-t asymptotic limit, and to divide the spin operators by the magnitude of the localized spin, j_1, so that the results for different j_1 values may be compared. Hence we define normalized correlation functions,

$$C_{yy}(t)=\{\langle S_y(0)S_y(t)\rangle-\langle S_y\rangle^2\}/(j_1)^2 , \tag{18}$$

with $C_{xx}(t)$ and $C_{zz}(t)$ being defined similarly.

The correlation functions are generically complex, but there are some interesting exceptions. For $B=0$, we find that $C_{xx}(t)$ and $C_{zz}(t)$ are complex but $C_{yy}(t)$ is real. To understand the latter, we substitute S_y for Q and R in (10)–(17). For a single step ($t=\tau$) the Heisenberg operator $S_y(\tau)$, reduced to the subspace of the localized spin, is given by the equivalent of (15),

$$S_y(\tau)=\mathrm{Tr}^{(b)}\{\rho_b U^\dagger S_y U\} . \tag{19}$$

This is invariant under rotations about the y axis, since the beam-particle state ρ_b is polarized in the y direction and the Hamiltonian (1), from which U is derived, has spherical symmetry for $B=0$. So a single step of (15) preserves the y-axis symmetry of $S_y(t)$ for $t=\tau$, and

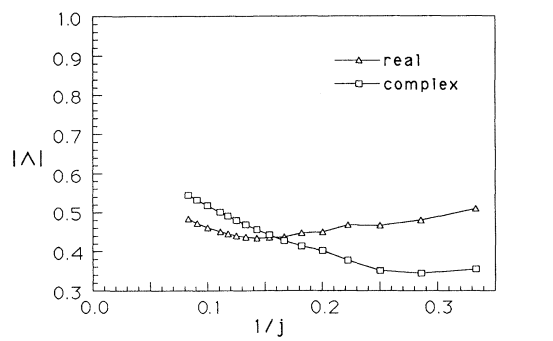

FIG. 7. Magnitudes of the subdominant real and complex eigenvalues (as in Fig. 3) vs $1/j$, for $j=j_1=j_2$, $aj_1=\pi$, $B=\pi$.

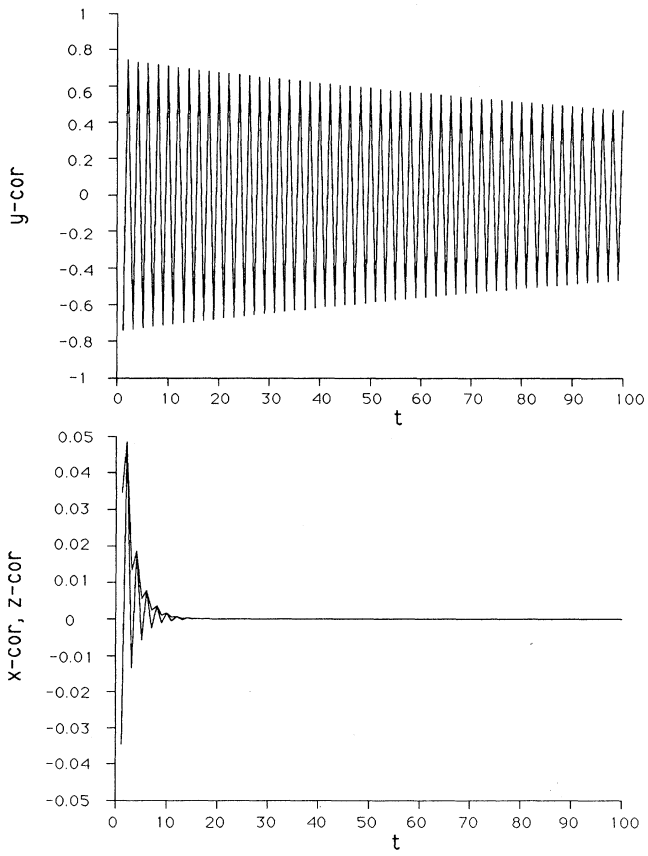

FIG. 8. Autocorrelation functions for $j_1=j_2=10$, $aj_1=\pi/2$, $B=\pi$. (Corresponding classical phase in Fig. 1 is $Y=\pm 1$.) Upper: $C_{yy}(t)$. Lower: real parts of $C_{xx}(t)$ (oscillatory curve) and $C_{zz}(t)$ (positive envelope).

hence n steps will also preserve the symmetry for $t=n\tau$. Therefore $S_y(0)$ and $S_y(t)$ will commute, and so (18) will be real.

For $B=\pi$ (in units of $\hbar=1$, $\tau=1$) the effect of the magnetic field is to rotate all spins about the z axis through an angle π. This reverses the sign of $S_y(t)$, but still preserves its rotational invariance about the y axis. Thus $C_{yy}(t)$ is also real in this case.

Qualitatively different autocorrelation functions are obtained for parameter values that correspond to different classical motions. Figure 8 corresponds to the phase labeled $Y=\pm 1$ in Fig. 1. The longitudinal correlation, $C_{yy}(t)$, oscillates strongly and is slightly damped. The damping is governed by the subdominant eigenvalue of Eq. (9), which approaches -1 as j_1 increases. In the limit $j_1\to\infty$ the oscillation of $C_{yy}(t)$ becomes undamped, in agreement with the stable pole-to-pole oscillation of the classical model. The transverse correlations, given by the real parts of $C_{xx}(t)$ and $C_{zz}(t)$, have small amplitudes and are strongly damped. Both the amplitude and the range of the transverse correlations diminish as j_1 increases.

For $B=\pi$, both $C_{xx}(t)$ and $C_{zz}(t)$ contain the same information, $C_{xx}(t)$ differing from $C_{zz}(t)$ by an additional factor of $(-1)^t$ because of the π rotation of spins about the z axis. (Here t is an integer because we set $\tau=1$.)

Figure 9 shows the longitudinal correlations for several models belonging to the chaos phase of Fig. 1. The strength of the correlation function gradually increases with the magnitude of the quantum spins. An extrapolation to $j=\infty$ was calculated, using six values of j (of which only three are shown in Fig. 9). The result is quite similar to the classical autocorrelation function, however, the latter has a significantly longer range. The transverse correlations (not shown) are much weaker than the longitudinal correlations for both classical and quantum models.

The parameters for Fig. 10 correspond to the phase 1 in Fig. 1, for which the y component of the classical spin converges to a unique value, while the x and z components move on a limit cycle transverse to the beam. For the final state of the quantum spin, the probability distribution of S_y has a single peak, and the distributions for S_x and S_z are very broad (see Fig. 16 of Ref. [2]). In this case, the longitudinal correlation function is very weak and very short ranged, implying that fluctuations within the narrow S_y distribution are essentially random. However, the transverse correlations are large and long ranged, describing the more orderly motion on the transverse limit cycle.

These results demonstrate that the main features of the three largest classical phases in Fig. 1 are realized by the quantum model for quite modest values of j_1 and j_2. But the classical phase 2, in which S_y has a period-2 limit cycle, could not be obtained for quantum spins as large as $j_1=14$; instead the results resembled those for whichever of the phases 1 or $Y=\pm 1$ was closer. Evidently, it will

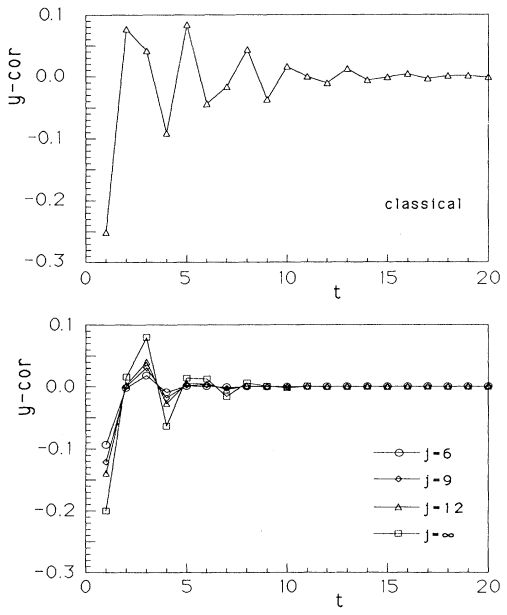

FIG. 9. Longitudinal autocorrelation function $C_{yy}(t)$ for the *chaos* phase ($j_1=j_2$, $aj_1=\pi$, $B=\pi$). Upper: classical model. Lower: quantum model for several j values, and extrapolation to $j=\infty$.

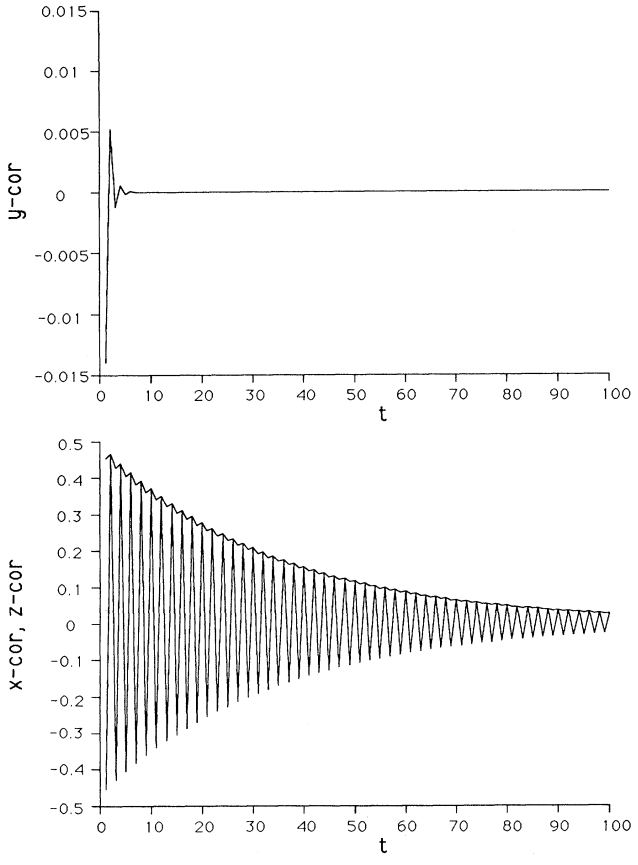

FIG. 10. Autocorrelation functions for $j_1=12$, $j_2=6$, $aj_1=1.5\pi$, $B=\pi$. (Corresponding classical phase in Fig. 1 is 1.) Upper: $C_{yy}(t)$. Lower: real parts of $C_{xx}(t)$ (oscillatory curve) and $C_{zz}(t)$ (positive envelope).

require very much larger values of j_1 in order to resolve the many phases that occur along the classical bifurcation route to chaos.

The imaginary parts of the corrrelation functions are related to the noncommutation of the time-dependent operators. For the phase $Y=\pm 1$, both the real and the imaginary parts of $C_{xx}(t)$ and $C_{zz}(t)$ are small, with the imaginary parts being smaller, but comparable in magnitude to the real parts. For the chaos phase, the imaginary parts are about 20 times smaller than the real parts. For the phase 1, the imaginary parts are 50–100 times smaller than the real parts. For $B=0.7\pi$ (discussed in detail in the next section), all three correlation functions are complex. The imaginary parts of $C_{xx}(t)$ and $C_{yy}(t)$ are about 100 times smaller than the real parts, while the imaginary part of $C_{zz}(t)$ is 5000 times smaller than the real part. In this case the magnitudes of the imaginary parts appear to decrease systematically as j increases, but no such trend was apparent for the chaos phase. Smallness of the imaginary parts makes it plausible to interpret the real parts as ordinary correlations (see Sec. II C), but the precise interpretation of complex correlation functions is not clear.

V. NONUNIQUE FINAL STATES

For certain values of the parameters, the classical model may have more than one attractor, and the final state will depend upon the initial state. Figure 11 shows a case with two quasiperiodic limit cycles. In Ref. [1] it was pointed out that the quantum model too can have nonunique final states, if the parameters are such that the eigenvalue $\Lambda=1$ in (9) is degenerate. However, the nonuniquenesses in the classical and quantum models are entirely unrelated.

As was explained in [1], the final quantum state is nonunique when the parameters are such that a certain phase shift is zero (mod2π), rendering the Hamiltonian ineffective in a certain subspace. Such a situation occurs for $B=0$, $a(j_1+j_2)=2\pi$, and as a result, the states $|j_1,j_1\rangle$ and $|j_1,j_1-1\rangle$ (and also superpositions and mixtures of them) are possible final states of the localized spin. However, the difference in polarization between these final states becomes insignificant in the limit $j_1\to\infty$. For the corresponding classical model, there is only one final steady state—the localized spin must align with the beam. Now, as was shown in [2], the effect of the interaction is to rotate the spins about the total angular momentum **J** through the angle aJ. If $a(j_1+j_2)=2\pi$, the rotation angle aJ approaches 2π as the localized spin approaches alignment. But a rotation through 2π has no effect, so the closer the spin comes to its final state, the less effective is the interaction in achieving that state. It can be shown that, instead of the usual exponential approach to perfect alignment, in this case the misalignment decays only as $t^{-1/2}$.

For parameter values corresponding to Fig. 11, the quantum model has a unique final state. The classical model, with its two basins of attraction and two steady states, is analogous to a system with a double-well potential. Tunneling between the two wells is possible in the quantum model, and this leads to a unique final state. The steady-state probability distributions for the components of the localized quantum spin are shown in Fig. 12. The broad distributions for S_x and S_y are similar to those obtained from the classical limit cycles. (The pronounced bias toward negative values of S_y, not evident in Fig. 11, becomes apparent when the picture is projected from different vantage points.) The S_z distribution shows some indication of a bimodal shape, becoming more pronounced as j_1 and j_2 increase, but it will require much larger j values for it to develop clearly.

The autocorrelation functions are multiperiodic for motions on each of the two classical attractors. The results in Fig. 13 are for the x component of spin; those for the y component are very nearly the same. It is evident

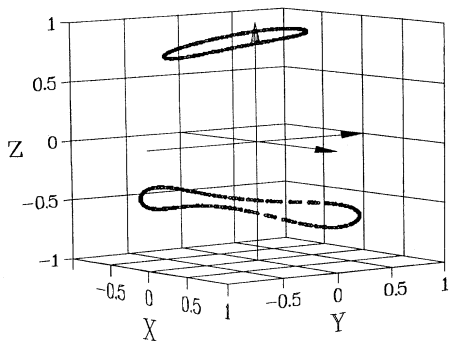

FIG. 11. Two classical attractors: $j_2/j_1=0.2$, $aj_1=\pi$, $B=0.7\pi$.

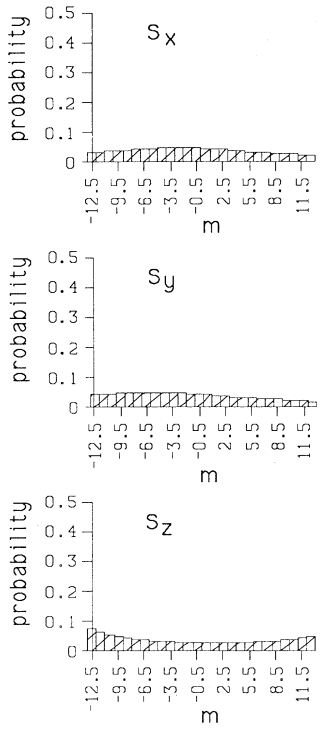

FIG. 12. Steady-state quantum spin distributions for $j_1=12.5$, $j_2=2.5$, $aj_1=\pi$, $B=0.7\pi$.

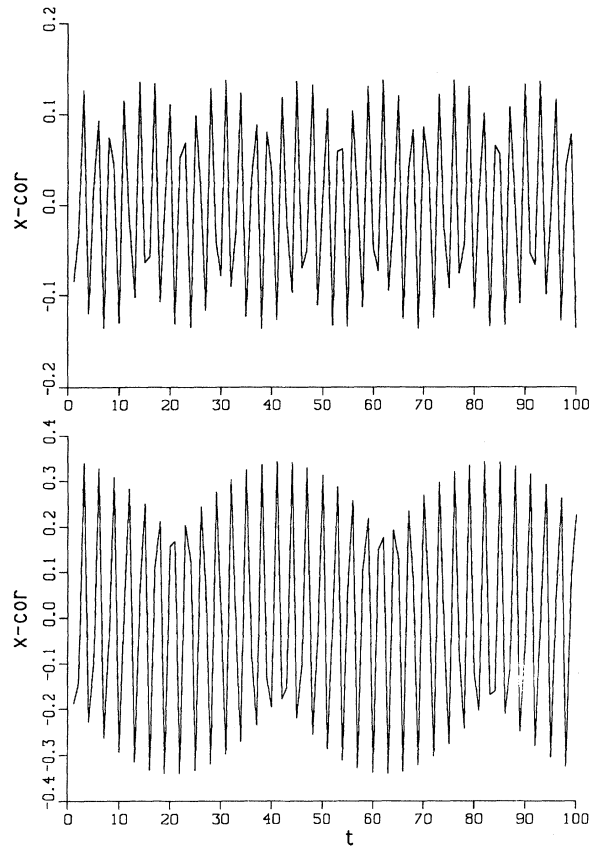

FIG. 13. Classical autocorrelation functions of the x component of spin, in the upper and lower attractors of Fig. 11.

that there is a rapid oscillation with period T_1, and a modulation with longer period T_2. In the upper attractor these periods are $T_1=2.81$ and $T_2=15.2$; in the lower attractor they are $T_1=2.96$ and $T_2=42.6$. The short period T_1 is the time for the spin to make a circuit around the limit cycle. T_2 corresponds to a near return

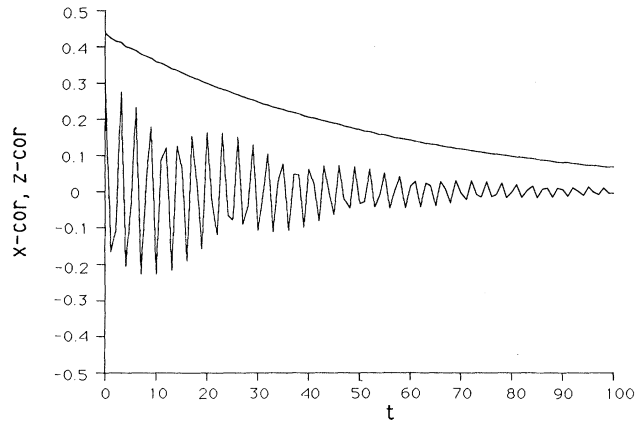

FIG. 14. Quantum autocorrelation functions for $j_1=12.5$, $j_2=2.5$, $aj_1=\pi$, $B=0.7\pi$. The upper, smooth curve is Re $C_{zz}(t)$; the lower, oscillatory curve is Re $C_{xx}(t)$.

of the spin to its initial value.

In the quantum model the autocorrelation functions $C_{xx}(t)$ and $C_{yy}(t)$ are also nearly identical. This is not guaranteed by any symmetry, so it must be interpreted as an indication of motion on a limit cycle. If the quantum steady state were, approximately, a mixture of the two classical limit cycles, then one would expect its autocorrelation function (Fig. 14) to exhibit all four of the periods described above. But instead it has periods $T_1=2.88$ and $T_2=24.4$, which are intermediate between those of the classical limit cycles. This indicates that the motions involving positive and negative S_z are not yet decoupled. However, the autocorrelation function for S_z (Fig. 14) is monotonic, indicating that S_z does not oscillate between positive and negative values. That is consistent with the corresponding classical behavior.

VI. CONCLUSIONS

This paper began with a paradox: the unique final state of the quantum model seemed to be incompatible with the variety of time-dependent steady states (limit cycles and chaos) of the classical model. An oscillatory classical orbit is not matched with an oscillatory quantum density matrix. The paradox is resolved by taking into account the essentially statistical nature of quantum states. The classical limit of a quantum state is generally an ensemble of classical orbits, not a single orbit (as was pointed out by Einstein to Born [11] many years ago; see also [12]). In Ref. [2] the analogous quantum and classical steady-state ensembles were shown to have similar statistical distributions, with the quantum probabilities apparently converging to the classical probabilities in the limit $j\rightarrow\infty$. In this paper we have seen that dynamical information is contained in autocorrelation functions, even though the quantum state function may be stationary. By varying the parameters of the Hamiltonian to correspond to different kinds of classical motions, we obtain qualitatively different quantum autocorrelation functions, which closely resemble their classical analogs.

The conjecture, according to which the limit $j\rightarrow\infty$ cannot be interchanged with the limit $t\rightarrow\infty$, has been confirmed and illustrated in terms of the limiting behavior of the eigenvalues of Eq. (9), which govern the dynamics of the quantum model. Surprisingly, the numerical data suggest that the conjecture may fail (i.e., the limits will commute) in the region of chaotic classical motion. However, that suggestion had better be taken with caution, as a challenge to investigate the asymptotic behavior of the eigenvalues in greater detail.

The physical significance of the mathematical fact, that the limits $j\rightarrow\infty$ and $t\rightarrow\infty$ are not commutative, is not self-evident. It is sometimes claimed, in studying the classical limit, that the order of limits, $t\rightarrow\infty$ after $j\rightarrow\infty$, is "right," whereas the opposite order, $j\rightarrow\infty$ after $t\rightarrow\infty$, is "wrong." If that claim were accepted literally, one might conclude that the quantal steady states obtained in [1], [2], and the present paper have no relevance to the classical steady state. But we have seen, very clearly, that such is not the case; the quantal steady states do have classical analogs, and seem to have the correct classical limits.

When, in physics, we discuss the limit of some parameter becoming infinite, we really mean that it is much larger that any comparable magnitude in the system. Thus, since j is dimensionless, the limit $j \to \infty$ means $j \gg 1$. But what does $t \to \infty$ mean? Is $t = 1992$ a "large" value? The question is meaningless, because the origin, $t = 0$, can be chosen arbitrarily. Usually, in quantum mechanics, $t = 0$ is taken to be the time of the initial-state preparation. But, in this model, every passage of a beam particle can be regarded as preparing *some* state of the localized spin. Moreover, the initial-state preparation is irrelevant, since (except for certain special parameter values) the final state is independent of the initial state. If one were to choose that final state initially, then the passage of only one beam particle would confirm that a steady state existed. Thus, for our model, the limit $t \to \infty$ (measuring t from the initial preparation) is inessential and irrelevant. This should serve as a warning against a simplistic interpretation of the right order of limits.

Although correlation functions arise naturally as basic entities in a dynamical theory, the situation is complicated because the quantum correlation functions are complex (except for cases having special symmetry). I have followed the usual procedure of taking their real parts (equivalent to symmetrizing the noncommuting operators), but that procedure lacks a fundamental justification. The imaginary parts were found to be smaller than the real parts, often (but not always) orders of magnitude smaller, which adds plausibility to the procedure used. But the old problem of giving a precise interpretation to the complex correlation functions of noncommuting operators now seems more urgent than ever.

[1] L. E. Ballentine, Phys. Rev. A **44**, 4126 (1991).
[2] L. E. Ballentine, Phys. Rev. A **44**, 4133 (1991).
[3] J. J. Slosser, P. Meystre, and S. L. Braunstein, Phys. Rev. Lett. **63**, 934 (1989); J. J. Slosser and P. Meystre, Phys. Rev. A **41**, 3867 (1990).
[4] J. Gea-Banacloche, Phys. Rev. Lett. **65**, 3385 (1990); Phys. Rev. A **44**, 5913 (1991); Opt. Commun. **88**, 531 (1992).
[5] A. O. Barut, Phys. Rev. **108**, 565 (1957); A. O. Barut, M. Bozic, and Z. Maric, Found. Phys. **18**, 999 (1988).
[6] J. E. G. Farina, Am. J. Phys. **45**, 1200 (1977). This paper gives a simple example in which the symmetrized correlation between the position and momentum operators arises, and is the natural analog of the corresponding classical correlation.
[7] M. C. Gutzwiller, *Chaos in Classical and Quantum Mechanics* (Springer-Verlag, New York, 1990).
[8] F. Haake, *Quantum Signatures of Chaos* (Springer-Verlag, Berlin, 1991).
[9] L. E. Reichl, Z-Y. Chen, and M. Millonas, Phys. Rev. Lett. **63**, 2013 (1989).
[10] M. V. Berry, Physica D **33**, 26 (1988).
[11] A. Einstein, *Scientific Papers Presented to Max Born* (Oliver and Boyd, Edinburgh/London, 1953).
[12] L. E. Ballentine, *Quantum Mechanics* (Prentice-Hall, Englewood Cliffs, NJ, 1990), Chap. 15.